Isı Bilimi ve Tekniği Dergisi, 37, 1, 127-137, 2017
J. of Thermal Science and Technology

ISSN 1300-3615

EMPIRICAL CORRELATIONS FOR THE PERFORMANCE OF AN AUTOMOTIVE AIR CONDITIONING SYSTEM USING R1234yf AND R134a

Mumin Celil ARAL*, Murat HOSOZ and Mukhamad SUHERMANTO*****
Department of Automotive Engineering, Kocaeli University, 41380 İzmit, Kocaeli
*mumincelilaral@yandex.com, **mhosoz@kocaeli.edu.tr, ***ahmad.herman@gmail.com

(Geliş Tarihi: 09.05.2016, Kabul Tarihi: 14.11.2016)

Abstract: A laboratory automotive air conditioning (AAC) system was set up and tested for the cases of employing refrigerants R134a and R1234yf. Two different empirical correlations were developed to predict the steady state performance parameters of the AAC system based on some experimental data. The air stream temperatures entering the evaporator and condenser and the relative humidity of the air stream at the evaporator inlet were selected as the input parameters of the proposed correlations, while the output parameters were the cooling capacity, power absorbed by the refrigerant in the compressor, condenser heat rejection rate, coefficient of performance, conditioned air temperature, compressor discharge temperature and the rate of total exergy destruction in the AAC system. Then, the predictions of these correlations were compared with the experimental results which were not used in developing the correlations. The findings suggest that both correlations can be used for accurately predicting the performance parameters of the AAC systems.
Keywords: Automotive, Air conditioning, R1234yf, R134a, Performance, Empirical.

R1234yf ve R134a KULLANAN BİR OTOMOTİV İKLİMLENDİRME SİSTEMİNİN PERFORMANSI İÇİN AMPİRİK KORELASYONLAR

Özet: Laboratuar amaçlı bir otomotiv iklimlendirme sistemi kurularak R134a ve R1234yf soğutucu akışkanlarının kullanılması durumları için testler gerçekleştirilmiştir. Sistemin sürekli rejim performans parametrelerini tahmin edebilmek amacıyla, deneysel sonuçların bir kısmı kullanılarak iki farklı ampirik bağıntı geliştirilmiştir. Söz konusu bağıntıların giriş parametreleri olarak evaporatör ile kondensere giren hava akımlarının sıcaklıkları ve evaporatör girişindeki hava akımı izafi nemi seçilmiştir. Çıkış parametreleri ise soğutma kapasitesi, kompresörde soğutucu akışkana verilen güç, kondenserden atılan ısı, soğutma tesir katsayısı, şartlandırılmış hava akımı sıcaklığı, kompresör çıkış sıcaklığı ve sistemde yok edilen toplam ekserji olarak belirlenmiştir. Daha sonra bağıntılar kullanılarak elde edilen tahminler, bağıntıların geliştirilmesi aşamasında kullanılmayan deneysel sonuçlar ile karşılaştırılmıştır. Her iki korelasyonun da taşıt iklimlendirme sistemlerinin performans parametrelerinin doğru bir şekilde tahmin edilmesinde kullanılabileceği sonucuna ulaşılmıştır.
Anahtar Kelimeler: Otomotiv, İklimlendirme, R1234yf, R134a, Performans, Ampirik.

NOMENCLATURE

a	actual
AAC	automotive air conditioning
c	constant coefficient
CFC	chlorofluorocarbon
COP	coefficient of performance
$c_{p,a}$	specific heat of air [kJ/kg K]
$c_{p,v}$	specific heat of water vapour [kJ/kg K]
d	constant coefficient
$\dot{E}x_d$	exergy destruction rate [kW]
F_1	output parameter predicted by the first correlation
F_2	output parameter predicted by the second correlation
GWP	global warming potential
h	specific enthalpy [kJ/kg]
HCFC	hydrochlorofluorocarbon
HFC	hydrofluorocarbon
k	constant coefficient
$\dot{m}$	mass flow rate [kg/s]
MRE	mean relative error [%]
N	total number of predicted data
ODP	ozone depletion potential
p	predicted
P	pressure [kPa]
$\dot{Q}_{evap}$	cooling capacity [kW]
$\dot{Q}_{cond}$	condenser heat rejection rate [kW]
$\dot{Q}_j$	heat transfer on the boundary of the control volume [kW]
R	correlation coefficient

R_a	ideal gas constant of air [kJ/kg K]
RMSE	root mean square error
s	specific entropy [kJ/kg K]
T	temperature [°C, K]
t_c	condensing temperature [°C]
t_e	evaporating temperature [°C]
T_j	boundary temperature [K]
TXV	thermostatic expansion valve
$\dot{W}_{comp}$	compressor power [kW]
$\dot{W}_{cv}$	work produced in the control volume [kW]
X	independent variable
Y	a function of independent variables

Greek symbols

ω	specific humidity ratio [kg water/kg air]
ϕ	relative humidity [%]
ψ	specific flow exergy [kJ/kg]

Subscripts

0	reference (dead) state
a	air
ai	air inlet
comp	compressor
cond	condenser
cv	control volume
dis	discharge
evap	evaporator
in	inlet
out	outlet
r	refrigerant
tot	total

INTRODUCTION

Automotive air conditioning (AAC) systems were first employed in 1930s with the development of car air conditioner using R12, which was a refrigerant from CFC family. AAC systems have been impressively improved in ways that causing less adverse impact on environment, providing a better thermal comfort in the passenger compartment and having less initial investment and operating costs (Bhatti, 1999).

Almost all current AAC systems utilise vapour compression refrigeration cycle driven by the engine crankshaft. The AAC systems differ from the residential air conditioning systems because they operate in transient state instead of steady state as a consequence of the continually changing engine speed (Hemami, 1999).

The Montreal Protocol in 1987 called for a restriction of the chemicals such as CFC and HCFC compounds including R12 due to their high ozone depletion potential (ODP). According to this protocol, CFCs would be entirely phased out in the developed countries starting from 1996 whereas in developing countries they should be totally removed in 2010 (UNEP, 1987). Therefore, R134a, which is a member of HFC family, has been used in AAC systems as alternative to R12 since 1994.

Although the refrigerants such as R134a, R410a, R407c and R404a are completely harmless for the ozone layer, they have high degrees of global warming potential (GWP). Since global warming has been seriously seized the world attention in recent years, a step on addressing ways to solve global warming was taken further by the proposal of Kyoto Protocol in 1997 to control not only high ODP gases but also those with high GWP. Moreover, some regulations concerning their usage have been put in order (Lee and Jung, 2012). According to these regulations, the use of R134a in AAC systems has been restricted down from 2017. Potential candidates as alternatives to R134a are CO_2, R152a, and R1234yf. Since CO_2 requires high system pressures and has relatively low efficiency, and in other respects, R152a has comparatively high flammability, R1234yf has been regarded as the best potential candidate (Wang, 2014).

Even though it is known that AAC systems rarely operate in steady state in practice, most of the previous investigations in this field were aimed at determining the steady state performance of AAC systems.

Vargas and Parise (1995) worked on a mathematical model that was able to obtain the performance of a heat pump system using variable capacity compressor. Alkan and Hosoz (2010a) compared experimental performance parameters of an R134a AAC system with a thermostatic expansion valve for the cases of using fixed and variable capacity compressors. They also presented comparative experimental performance of an R134a AAC system for two different types of expansion devices, namely thermostatic expansion valve and orifice tube (Alkan and Hosoz, 2010b).

Kiatsiriroat and Euakit (1997) worked on a refrigeration cycle of an AAC system using R22/R124/R152, and used mathematical models developed for each component in order to simulate the system.

Hosoz and Direk (2006) developed an automotive air-to-air heat pump system, and compared its experimental heating and cooling mode performance parameters. Hosoz and Ertunc (2006) developed an artificial neural network (ANN) model to predict the performance of an AAC system using R134a.

Belman-Flores and Ledesma (2015) performed a statistical analysis for the energy performance of a vapour compression refrigeration cycle of an AAC system using R1234yf.

Yataganbaba et al. (2015) performed theoretical exergy analysis of a simple vapour compression refrigeration system with single and dual evaporators using R1234yf and R1234ze in replacement to R134a, determining that R1234yf and R1234ze could be good replacements of R134a.

Navarro-Esbri et al. (2013) compared the energy performance of R134a and R1234yf in a monitored vapour compression system with an internal heat exchanger under a wide range of working conditions. Qi (2015) studied the performance improvement potentials of an R1234yf AAC system under various operating conditions by considering the effects of superheat at evaporator outlet, subcooling at condenser outlet and compressor efficiencies on the system performance.

As seen from the literature survey outlined above, there are numerous experimental studies to evaluate the performance parameters of AAC systems by using different refrigerants or different system components. However, the correlations for the steady state performance parameters of AAC systems operating at different compressor speeds and evaporator/condenser air inlet temperatures have not been studied yet.

In this study, empirical correlations for the steady state performance parameters of an experimental AAC system were developed for the cases of using both R134a and R1234yf. Then, the predictions of these correlations were compared with the experimental performance parameters, and a statistical performance analysis of the prediction results was carried out.

EXPERIMENTAL SETUP AND TEST PROCEDURE

The experimental setup was a bench top AAC system consisting of original components from an R134a AAC system belonging to a compact car. In addition, some extra components and instruments were employed to conduct the experiments under the required conditions and to perform mechanical measurements.

The photo and schematic illustration of the experimental AAC system are shown in Figures 1 and 2, respectively. It mainly consists of a five-cylinder swash plate compressor, a parallel-flow micro-channel condenser, a laminated type evaporator, a receiver/filter/drier and a thermostatic expansion valve (TXV).

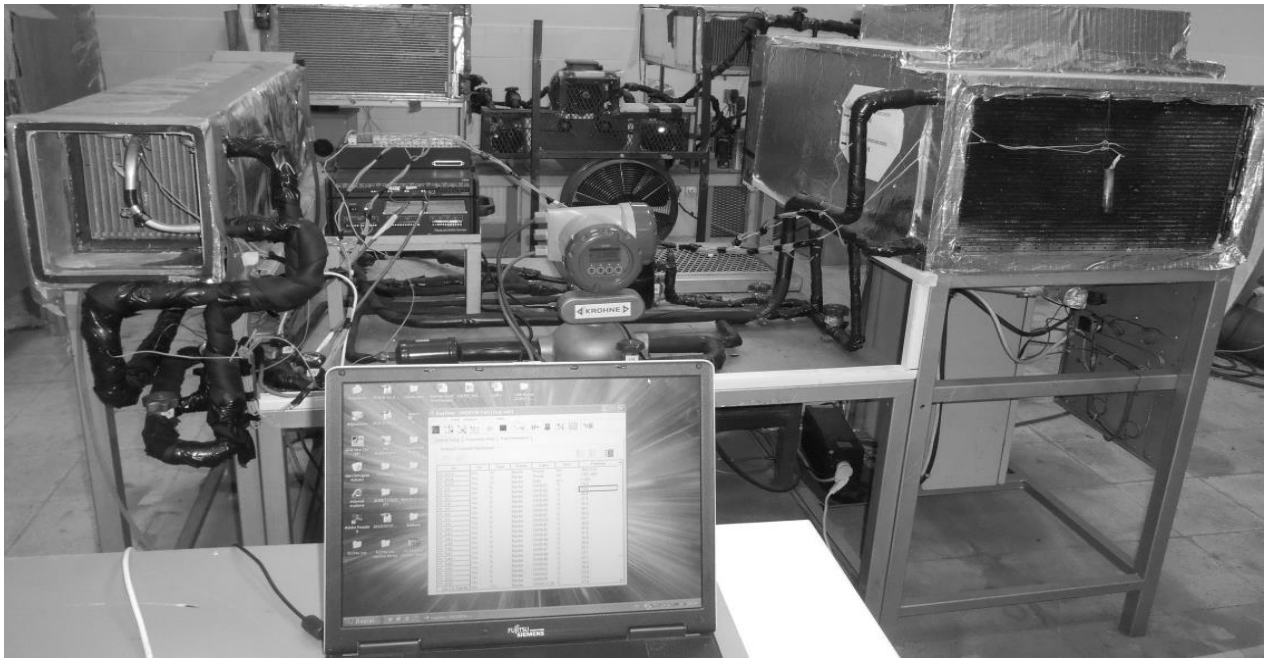

Figure 1. Photograph of the experimental AAC system.

The condenser and evaporator were inserted into 1-meter-long different air ducts with flow areas of 0.2345 m^2 and 0.0576 m^2, respectively. In order to provide the condenser air stream, an axial fan was attached to the inlet of the condenser air duct providing an air flow rate of 0.182 $m^3\ s^{-1}$.

On the other hand, a centrifugal fan was attached to the inlet of the evaporator air duct providing an air flow rate of 0.112 $m^3\ s^{-1}$. In order to determine the volume flow rates of the condenser and evaporator air streams, the air flow speeds at the outlets of condenser and evaporator were measured at many locations using an anemometer. Then, they were averaged and transferred into the continuity equation together with the outlet flow areas. Seperate electric heaters were installed in the upstream of condenser and evaporator air ducts, which could be energized in the ranges of $0-6$ kW and $0-2$ kW, respectively, to test the system at required air temperatures.

Voltage regulators were used to control the required air inlet temperatures at the inlets of the condenser and evaporator. The compressor was driven by a three phase electric motor via a frequency inverter to operate the system at various speeds, which were set by controlling the output frequency of the inverter.

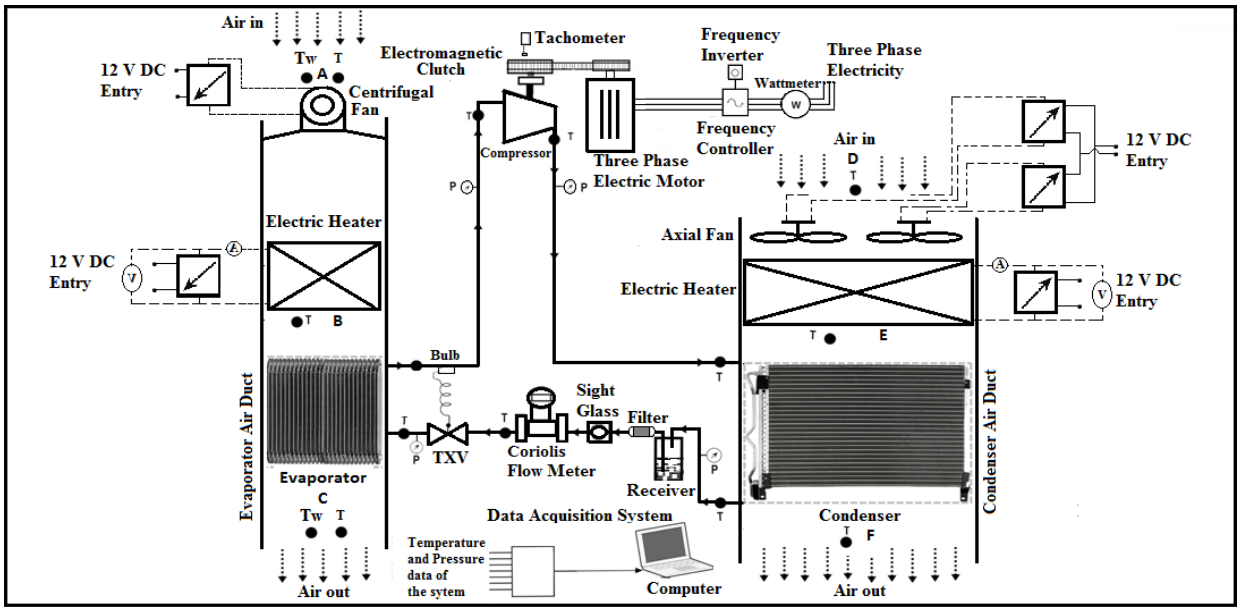

Figure 2. Sketch of the experimental AAC system.

In the experimental AAC system, the refrigerant is pulled into the compressor as low pressure superheated vapour, compressed to high pressure superheated vapour and sent into the condenser. After desuperheating, condensing and subcooling in the condenser, the refrigerant leaves it as high pressure subcooled liquid. Then, upon passing through the TXV, it undergoes pressure reduction and accompanying temperature drop. As a result, the refrigerant turns into a mixture of saturated liquid and saturated vapour at the inlet of the evaporator. The bulb of the TXV senses the refrigerant temperature at the evaporator outlet, and the TXV adjusts the refrigerant mass flow rate to keep the superheat at the evaporator outlet constant at a predetermined value. Next, the refrigerant evaporates by absorbing heat from the conditioned air stream, and leaves the evaporator as low pressure superheated vapour. Finally, it goes back to the compressor, thus completing the cycle.

All piping of the refrigeration circuit was made of copper tubing insulated by elastomeric-insulator. Using service station, the AAC system was first charged with R134a when the system was operated at 800 rpm compressor speed and 40 °C air stream temperature at the evaporator and condenser inlets. When the bubbles in the sight glass disappeared, the charging process was finished, and tests were performed. The R134a charged into the system was 2.20 kg, which was higher than the charge of a normal AAC system due to the extra pipeline used in the system to operate it as a heat pump in winter season. After R134a tests, the refrigerant in the system was recovered, the system was evacuated, charged with R1234yf, and the tests were repeated. The R1234yf charge was determined similar to the method used for determining R134a charge. The amount of R1234yf charge was found as 2.00 kg. The oil used in the system for both refrigerants was approximately 0.5 kg of PAG oil.

The compressor speed was measured by a photoelectric tachometer. The refrigerant mass flow rate was measured by a Coriolis mass flow meter located in the liquid line. The condenser and evaporator pressures were measured by both Bourdon type manometers and pressure transmitters.

The refrigerant temperature and air dry/wet bulb temperatures were measured at the inlet and outlet of each important component by type-K thermocouples. Measured variables were usually acquired through a data acquisition system having 16 bit − 200 KHz frequency with a 56 channel thermocouple input module, and recorded on a computer. The characteristics of the instrumentation and specifications of the compressor used in the experimental system are shown in Tables 1 and 2, respectively.

Table 1. Characteristics of the instrumentation.

Measured Variable	**Instrument**	**Range**	**Accuracy**
Temperature	Type-K thermocouple	-50 to 500 °C	± 0.5 °C
Pressure	Pressure transmitter Bourdon gauge	0 to 25 bar -1 to 10, 0 to 30 bar	± 0.2 % full scale 0.1, 0.5 bar
Air flow speed	Anemometer	0.1 to 15 m s-1	± 3.0 % reading
Refrigerant mass flow rate	Coriolis flow meter	0 to 350 kg h-1	± 0.1 % full scale
Compressor speed	Photoelectric tachometer	10 to 99999 rpm	± 0.1 % reading +2 rpm

Table 2. Specifications of the compressor.

Model	SD5H14
Max. speed (rpm)	6000
Outlet pressure (kPa)	1670
Intake pressure (kPa)	196
Number of cylinders	5
Cylinder volume (cc)	138
Weight (kg)	7.8
Designed for	R134a

The experimental system was tested at four different compressor speeds between 1000 and 2500 rpm with intervals of 500 rpm. At each speed, the air temperature entering the evaporator ($T_{evap,ai}$) was changed between 25 and 40 °C with intervals of 5 °C, while the air temperature entering the condenser ($T_{cond,ai}$) was changed between the selected $T_{evap,ai}$ and 40 °C with intervals of 5 °C. On the other hand, the relative humidity of the air stream entering the evaporator varied between 25% and 64%. Consequently, 40 tests for each refrigerant were performed. Each test took 15 minutes, and the steady state test data were employed in the evaluations. It was assumed that the steady state was achieved when the temperature deviations at the key points considered were within 0.5 °C for 3 minutes. The thermodynamic properties of refrigerants were obtained from commercial software as a function of the temperature and pressure.

THERMODYNAMIC ANALYSIS

In order to determine the steady state performance parameters of the experimental AAC system, the first law of thermodynamics was applied to each component of the refrigeration circuit.

The changes in kinetic and potential energies were neglected, and it was assumed that there was no pressure drop in the refrigerant lines as well as in the evaporator and the condenser. Then, the cooling capacity of the evaporator can be evaluated from

$$\dot{Q}_{evap} = \dot{m}_r (h_{evap,out} - h_{evap,in}) \quad (1)$$

where $h_{evap,out}$ and $h_{evap,in}$ are the refrigerant specific enthalpies at the outlet and inlet of the evaporator, respectively, and $\dot{m}_r$ refers to the refrigerant mass flow rate.

Assuming that the compression process is adiabatic, the compressor power absorbed by the refrigerant can be determined from

$$\dot{W}_{comp} = \dot{m}_r (h_{comp,out} - h_{comp,in}) \quad (2)$$

where $h_{comp,out}$ and $h_{comp,in}$ are the refrigerant specific enthalpies at the outlet and inlet of the compressor, respectively.

The coefficient of performance for the system reveals its energetic performance, and it is defined as the ratio between the cooling capacity and compressor power, i.e.

$$COP = \frac{\dot{Q}_{evap}}{\dot{W}_{comp}} \quad (3)$$

The heat rejected from the condenser can be evaluated from

$$\dot{Q}_{cond} = \dot{m}_r (h_{cond,in} - h_{cond,out}) \quad (4)$$

where $h_{cond,in}$ and $h_{cond,out}$ are the refrigerant specific enthalpies at the inlet and outlet of the condenser, respectively.

The locations and magnitudes of the thermodynamic inefficiencies can be determined by performing an exergy analysis of the system using the general form of exergy rate balance equation for control volumes given below (Ozgener and Hepbasli, 2007)

$$\dot{E}x_d = \sum \left(1 - \frac{T_0}{T_j}\right) \dot{Q}_j - \dot{W}_{cv} + \sum \dot{m}_{in} \psi_{in} - \sum \dot{m}_{out} \psi_{out} \quad (5)$$

where $\dot{Q}_j$ is the time rate of heat transfer at the location on the boundary where the instantaneous temperature is T_j, $\dot{W}_{cv}$ is the work produced in the control volume, ψ is the flow specific exergy, T_0 is the environmental temperature representing the dead state, and $\dot{E}x_d$ is the rate of exergy destruction in the control volume.

The specific flow exergy can be determined from

$$\psi = h - h_0 - T_0 (s - s_0) \quad (6)$$

where subscript "0" represents reference (dead) state.

The rate of exergy destruction in the adiabatic compressor, which is due to gas friction, mechanical friction and internal heat transfer, can be evaluated from

$$\dot{E}x_{d,comp} = \dot{m}_r \left(\psi_{comp,in} - \psi_{comp,out}\right) + \dot{W}_{comp} \quad (7)$$

The rate of exergy destruction in the condenser, which is due to heat transfer between refrigerant and air streams, can be obtained from

$$\dot{E}x_{d,cond} = \dot{m}_r \left(\psi_{cond,in} - \psi_{cond,out}\right) + \dot{m}_{a,cond} \left(\psi_E - \psi_F\right) \quad (8)$$

where $\dot{m}_{a,cond}$ is the mass flow rate of the condenser air stream.

The specific flow exergies of air in Eq. (8) at locations E and F can be calculated from (Ozgener and Hepbasli, 2007)

$$\psi_a = \left(c_{p,a} + \omega c_{p,v}\right) T_0 \left(\frac{T}{T_0} - 1 - \ln\frac{T}{T_0}\right) + \left(1 + 1.6078\,\omega\right) R_a T_0 \ln\frac{P}{P_0} + R_a T_0 \left(1 + 1.6078\,\omega\right) \ln\frac{1 + 1.6078\,\omega_0}{1 + 1.6078\,\omega} + R_a T_0 1.6078\,\omega \ln\frac{\omega}{\omega_0} \quad (9)$$

where $c_{p,a}$ is the specific heat of air, $c_{p,v}$ is the specific heat of water vapour, R_a is ideal gas constant of dry air and ω is specific humidity.

Assuming that the thermostatic expansion valve operates adiabatically, the rate of exergy destruction in the TXV can be determined from

$$\dot{E}x_{d,TXV} = \dot{m}_r \left(\psi_{TXV,in} - \psi_{TXV,out}\right) \quad (10)$$

Using Eq. (6) for specific flow exergies and considering that enthalpy remains constant in the TXV, Eq. (10) yields

$$\dot{E}x_{d,TXV} = \dot{m}_r T_0 \left(s_{TXV,in} - s_{TXV,out}\right) \quad (11)$$

where $s_{TXV,in}$ and $s_{TXV,out}$ are the refrigerant specific entropies at the inlet and outlet of the TXV, respectively.

The rate of exergy destruction in the evaporator, which is due to the heat transfer between the air and refrigerant streams, can be evaluated from

$$\dot{E}x_{d,evap} = \dot{m}_r \left(\psi_{evap,in} - \psi_{evap,out}\right) + \dot{m}_{a,evap} \left(\psi_B - \psi_C\right) \quad (12)$$

The specific flow exergies of air in Eq. (12) at locations B and C can be obtained from Eq. (9).

Finally, the rate of total exergy destruction in the AAC system can be determined by summing up the exergy destructions in the components, i.e.

$$\dot{E}x_{d,tot} = \dot{E}x_{d,comp} + \dot{E}x_{d,cond} + \dot{E}x_{d,TXV} + \dot{E}x_{d,evap} \quad (13)$$

UNCERTAINTY ANALYSIS

The uncertainty of each calculated output parameter of the experimental AAC system, namely the cooling capacity, compressor power, *COP*, condenser heat rejection rate and the rate of total exergy destruction in the AAC system, was determined using the method suggested by Moffat (1988). This method assumes that the function Y is to be calculated from a set of totally N measurements (independent variables) represented by

$$Y = Y\left(X_1, X_2, ..., X_N\right) \quad (14)$$

The uncertainty of the result Y can be determined by combining the uncertainties of the individual terms using a root-sum-square method as given below.

$$\Delta Y = \left[\sum_{i=1}^{N} \left(\frac{\partial Y}{\partial X_i} \Delta X_i\right)^2\right]^{1/2} \quad (15)$$

Using the accuracies for the measured variables reported in Table 1 and evaluating Eqs. (1)–(13) in Eq.(15), the uncertainties of the calculated parameters were determined. The total uncertainties of $\dot{Q}_{evap}$, $\dot{W}_{comp}$, *COP*, $\dot{Q}_{cond}$ and $\dot{E}x_{d,tot}$ were estimated as 2.6 %, 2.8 %, 4.1 %, 3.0 % and 5.9 %, respectively.

EMPIRICAL CORRELATIONS FOR THE PERFORMANCE PARAMETERS

When the evaporating and condensing temperatures are regarded as input parameters, the following empirical equations are suggested by the Stoecker (1982) for the cooling capacity, compressor power and condenser load of a vapour compression refrigeration cycle, respectively.

$$\dot{Q}_{evap} = c_1 + c_2 t_e + c_3 t_e^{\,2} + c_4 t_c + c_5 t_c^{\,2} + c_6 t_e t_c + c_7 t_e^{\,2} t_c + c_8 t_e t_c^{\,2} + c_9 t_e^{\,2} t_c^{\,2} \quad (16)$$

$$\dot{W}_{comp} = d_1 + d_2 t_e + d_3 t_e^{\,2} + d_4 t_c + d_5 t_c^{\,2} + d_6 t_e t_c + d_7 t_e^{\,2} t_c + d_8 t_e t_c^{\,2} + d_9 t_e^{\,2} t_c^{\,2} \quad (17)$$

$$\dot{Q}_{cond} = \dot{Q}_{evap} + \dot{W}_{comp} \quad (18)$$

where t_e and t_c are evaporating and condensing temperatures, respectively, while c_i and d_i refer to constant coefficients. However, the input parameters for the considered experimental AAC system are the compressor speed, inlet temperatures of the evaporator and condenser air streams and relative humidity of the air at the inlet of the evaporator. Since the speeds and flow rates of the air streams passing over the evaporator and condenser were maintained constant, they were not selected as input parameters. As a function of the input parameters, two different empirical correlations were developed to evaluate the output parameters, namely the cooling capacity, conditioned air temperature, condenser heat rejection rate, compressor power, compressor discharge temperature and total exergy destruction in the AAC system.

General forms of these correlations are as follows

$$F_1 = c_1 + c_2 T_{evap,ai} + c_3 T_{cond,ai} + c_4 T_{evap,ai} T_{cond,ai} + c_5 T_{evap,ai}^{\,2} + c_6 T_{cond,ai}^{\,2} + c_7 T_{evap,ai}^{\,2} T_{cond,ai}^{\,2} + c_8 \phi_{evap,ai} + c_9 \phi_{evap,ai}^{\,2} \quad (19)$$

$$F_2 = k_1 + k_2 T_{evap,ai} + k_3 T_{cond,ai} + k_4 \phi_{evap,ai} + k_5 T_{evap,ai}^{\,2} + k_6 T_{cond,ai}^{\,2} + k_7 \phi_{evap,ai}^{\,2} + k_8 T_{evap,ai} T_{cond,ai} \phi_{evap,ai} + k_9 T_{evap,ai}^{\,2} T_{cond,ai}^{\,2} \phi_{evap,ai}^{\,2} \quad (20)$$

where c_i and k_i are constant coefficients and $\phi_{evap,ai}$ is the relative humidity of the air stream at the inlet of the evaporator, while F_1 and F_2 indicate any of the output parameters. The c_i and k_i coefficients in these correlations were calculated individually for each compressor speed.

The output parameters mentioned above were evaluated separately for both refrigerants, namely R134a and R1234yf. When determining the coefficients yielding best results, the results of one out of the ten temperature combination tests were excluded for each refrigerant and compressor speed, and the roots of the related empirical correlations were obtained by using the results of remaining nine temperature combination tests. The temperature combination yielding the closest prediction results to the experimental values was determined for each operating speed, and the results of this combination were used in the comparison. As a result, totally 16 different empirical correlations (8 as F_1 and 8 as F_2) were developed for each output parameter involving four different operating speeds and two different refrigerants. Furthermore, the *COP* was determined by dividing the predicted cooling capacity to the predicted compressor power prediction.

STATISTICAL PERFORMANCE OF THE EMPIRICAL CORRELATIONS

Three different statistical performance parameters were used to determine the accuracy of the predictions of the correlations.

The mean relative error (*MRE*), which indicates the mean percentage difference between the actual (experimental) and the predicted values, can be determined from

$$MRE\,(\%) = \frac{1}{N}\sum_{i=1}^{N}\left|100\frac{a_i - p_i}{a_i}\right| \tag{21}$$

where a_i, p_i and N stand for the actual values obtained from the experiments, predicted values determined by the empirical correlations and total number of predicted data, respectively.

The root mean square error (*RMSE*) can be calculated from

$$RMSE = \sqrt{\frac{1}{N}\sum_{i=1}^{N}\left(a_i - p_i\right)^2} \tag{22}$$

The correlation coefficient is a statistical performance criterion that is used to demonstrate the relation between the variables. This coefficient between the predictions obtained from empirical correlations and experiments is defined as follows (Holman, 2012)

$$R = \frac{N\sum_{i=1}^{N}a_i p_i - \left(\sum_{i=1}^{N}a_i\right)\left(\sum_{i=1}^{N}p_i\right)}{\left[N\sum_{i=1}^{N}a_i^{\,2} - \left(\sum_{i=1}^{N}a_i\right)^2\right]^{1/2}\left[N\sum_{i=1}^{N}p_i^{\,2} - \left(\sum_{i=1}^{N}p_i\right)^2\right]^{1/2}} \tag{23}$$

RESULTS AND DISCUSSION

The results of the two correlations expressed in Eqs. (19) and (20) are compared with the experimental performance parameters, and the comparison results are shown in Figures 3–9. All graphics are provided with a straight line indicating prefect prediction and the values of the statistical performance indicators.

Figure 3 indicates the comparison of the predicted and experimental cooling capacities for both refrigerants. Predictions obtained from correlation F_1 are closer to the experimental results compared with the predictions of correlation F_2. In addition, it is seen that both correlations give better results for the case of using R134a in the system.

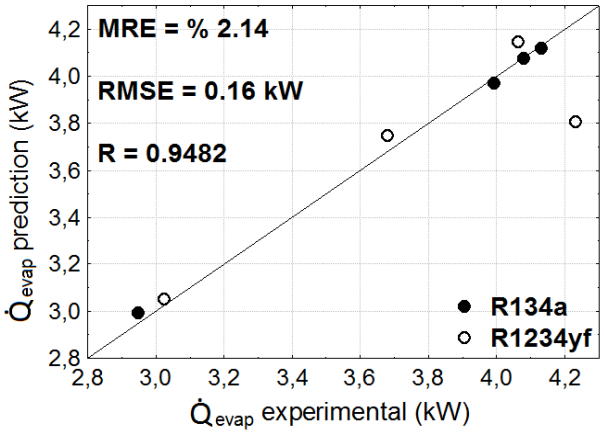

(a) Correlation F_1

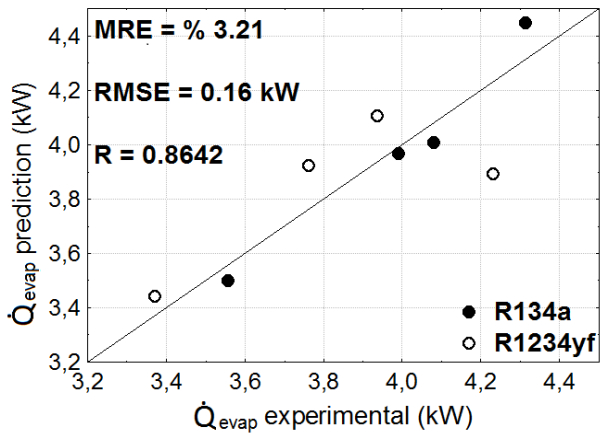

(b) Correlation F_2

Figure 3. Prediction results of empirical correlations for cooling capacity.

Figure 4 shows the comparison of the predicted and experimental compressor power for both refrigerants. The predicted $\dot{W}_{comp}$ values obtained from correlation F_2 have better statistical performance with a higher correlation coefficient along with lower *MRE* and *RMSE* values. It is seen that both correlations yield more accurate predictions when the system is operated with R134a.

Figure 5 illustrates the comparison of the predicted and experimental coefficient of performance values for both refrigerants. Note that *COP* predictions were not directly obtained from the correlations. Instead, they were evaluated from the predictions of cooling capacity and related compressor power. It is seen that F_1 predictions are closer to experimental results compared with F_2 predictions. Both correlations yield about the same accuracy for the refrigerants R134a and R1234yf.

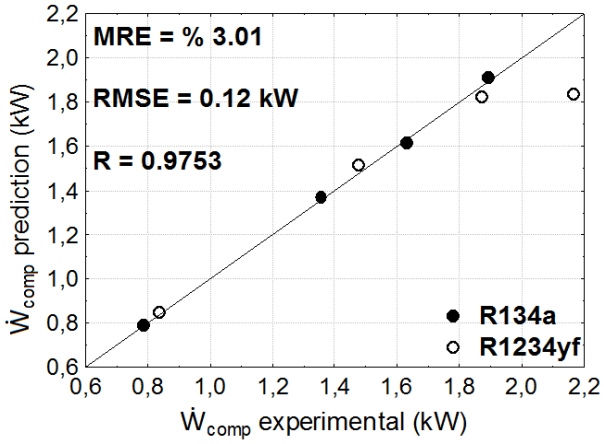

(a) Correlation F_1

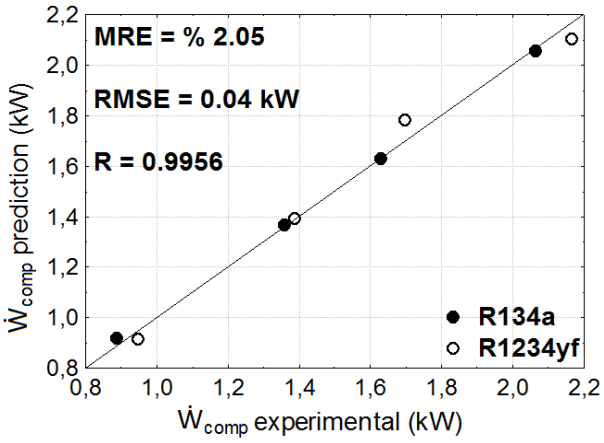

(b) Correlation F_2

Figure 4. Prediction results of empirical correlations for compressor power.

Figure 6 reports the comparison of the predicted and experimental condenser heat rejection rates for both refrigerants. It is seen that the predictions of both correlations yield almost the same correlation coefficient while predictions of F_2 have slightly better *MRE* and *RMSE* values.

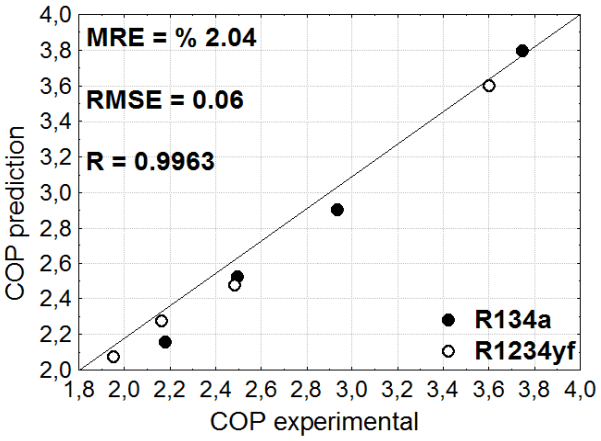

(a) Correlation F_1

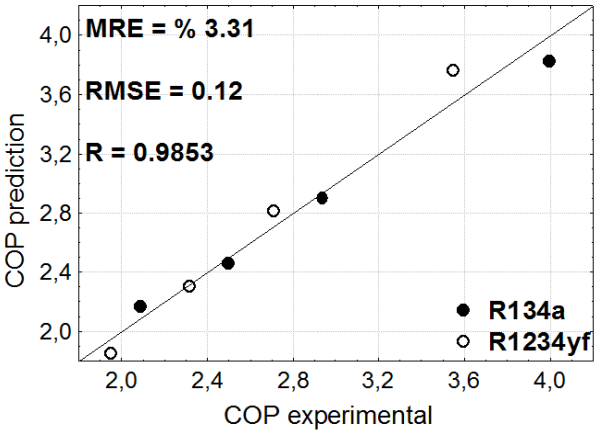

(b) Correlation F_2

Figure 5. Prediction results of empirical correlations for coefficient of performance.

Although the compressor discharge temperature is not considered as significant as other performance parameters of an AAC system, it must be followed for the compressor longevity. As the compressor discharge temperature increases, the compressor oil starts to lose its lubricating property. Furthermore, high compressor discharge temperatures cause excessive wear and reduction in compressor longevity. Figure 7 indicates the comparison of the predicted and experimental compressor discharge temperatures for both refrigerants. The predictions of F_2 yield better statistical performance with a correlation coefficient of 0.9967, a *MRE* of 1.12 % and a *RMSE* of 1.22 °C.

Another significant performance parameter of an AAC system is the air temperature leaving the evaporator. Figure 8 shows the comparison of the predicted and experimental air temperature at the evaporator outlet for both refrigerants. It is seen that the evaporator outlet temperature predictions of correlation F_1 yields better statistical performance with a correlation coefficient of 0.9716, a *MRE* of 2.89% and a *RMSE* of 0.49 °C. Although F_2 yields a correlation coefficient of 0.8832, it results in *MRE* and *RMSE* values of %3.48 and 0.66 °C, respectively, which may be regarded as quite accurate results.

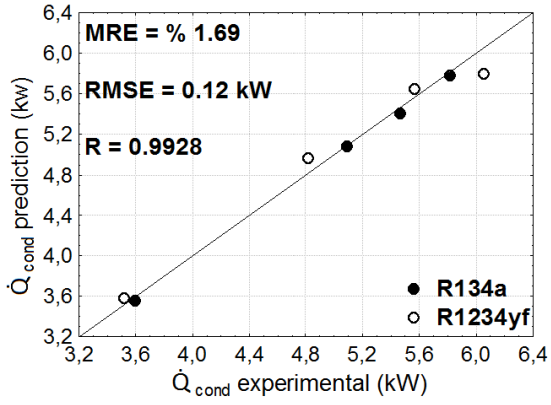

(a) Correlation F_1

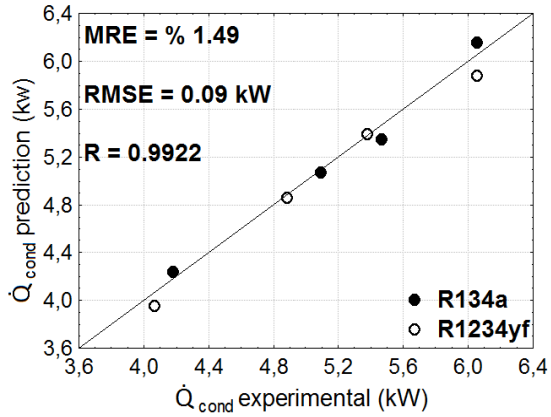

(b) Correlation F_2

Figure 6. Prediction results of empirical correlations for condenser heat rejection rate.

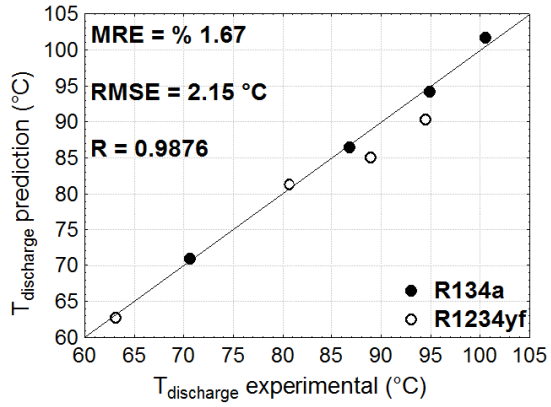

(a) Correlation F_1

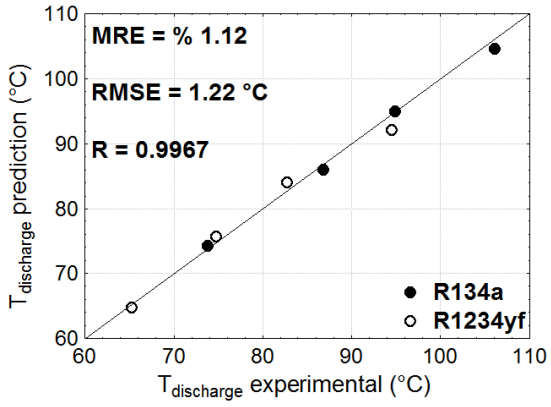

(b) Correlation F_2

Figure 7. Prediction results of empirical correlations for compressor discharge temperature.

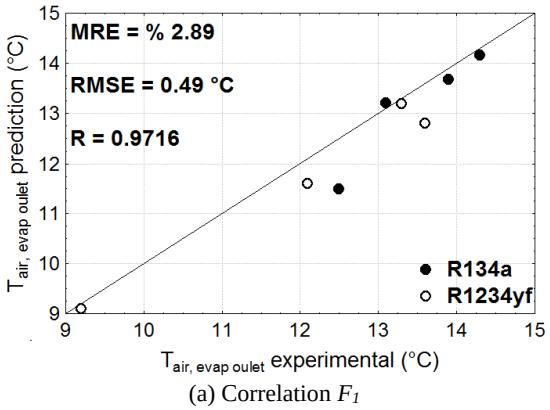

(a) Correlation F_1

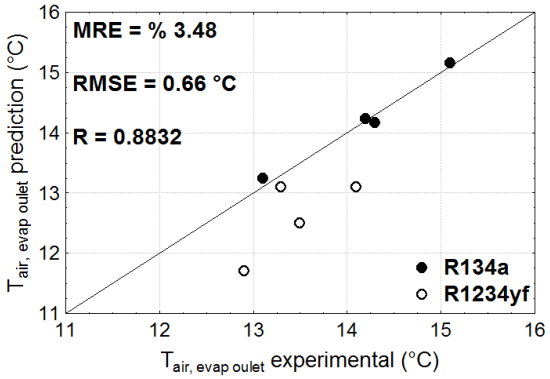

(b) Correlation F_2

Figure 8. Prediction results of empirical correlations for air temperature at the evaporator outlet.

Finally, Figure 9 shows the comparison of the predicted and experimental rates of total exergy destruction in the AAC system for both refrigerants. Although both correlations yield predictions with high statistical performance especially for the case of using R134a, the F_2 correlation is slightly better in predicting the rate of total exergy destruction.

As seen above, the results of the empirical correlations aimed in this study revealed a good agreement with the results reported in similar studies, which were performed using different methods (Atik et al., 2010; Hosoz et al., 2013; Kamar et al., 2013) such as ANN and ANFIS modeling techniques.

Atik et al. (2010) carried out a modeling of an R134a mobile air conditioning system with different amounts of refrigerant for different compressor speeds by using ANNs. They have found similar coefficient of correlation values, namely 0.945 for cooling capacity, 0.985 for compressor power and 0.994 for *COP*. Likewise, Hosoz et al. (2013) predicted the performance parameters of an R134a AAC system using ANFIS technique. They considered the air dry bulb temperature at the evaporator outlet, cooling capacity, coefficient of performance and the rate of total exergy destruction in the refrigeration circuit of the system as the output parameters of their model. Their ANFIS model yielded correlation coefficients in the range of 0.966−0.988 and *MRE* values in the range of 0.23−5.28 %, which were slightly poorer than the accuracy of the F_1 and F_2

correlations presented in this study. Moreover, Kamar et al. (2013) predicted the cooling capacity, compressor power input and *COP* of an AAC system by developing an ANN model. Their model also yielded less accurate results in comparison to the predictions of the present study. On the other hand, neither R1234yf nor the suggested empirical correlations were used in the previous studies.

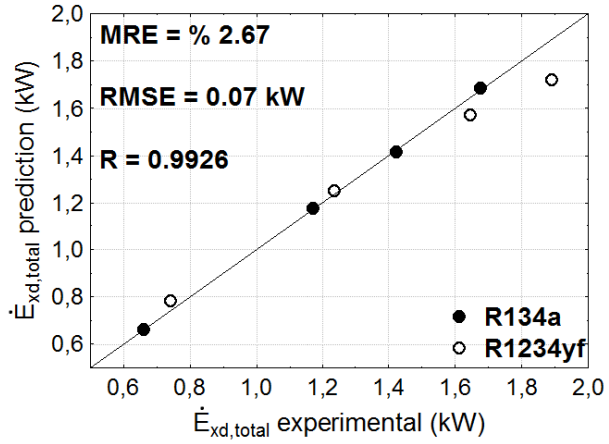

(a) Correlation F_1

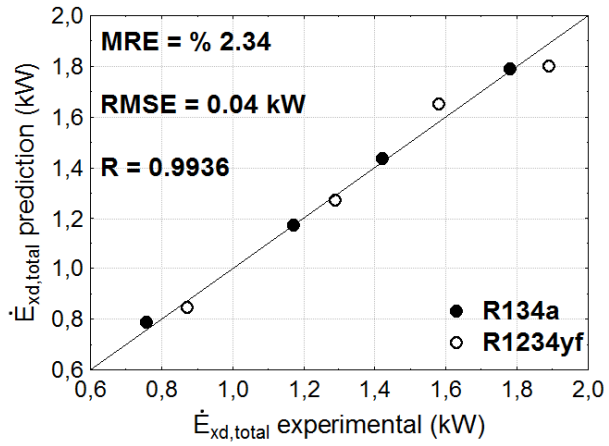

(b) Correlation F_2

Figure 9. Prediction results of empirical correlations for total exergy destructed in the AAC system.

CONCLUSIONS

An experimental AAC system using R134a and R1234yf was set up and tested under various operating conditions. Then, two different forms of empirical correlations were developed in order to predict the performance parameters of the AAC system based on experimental results. The predictions obtained from the empirical correlations were cooling capacity, compressor power, coefficient of performance, condenser heat rejection rate, compressor discharge temperature, air temperature at the evaporator outlet and the rate of total exergy destruction in the AAC system. The prediction results were compared with experimental ones, and the statistical performance of the predictions was determined in terms of correlation coefficient, mean relative error and root mean square error. The main findings are as follows:

The predictions of the correlation F_1 for the performance parameters of the AAC system yielded correlation coefficients within the range of 0.9482–0.9963, mean relative errors within the range of 1.67–3.01% and quite low root mean square errors. On the other hand, the predictions of the correlation F_2 yielded correlation coefficients within the range of 0.8642–0.9967, *MRE*s within the range of 1.12–3.48% and *RMSE*s comparable to those of F_1 correlations.

When all statistical performance criterions are taken into account, correlation F_1 can be utilized for predicting the cooling capacity, coefficient of performance and air temperature at the evaporator outlet, while correlation F_2 can be used for predicting the compressor power and compressor discharge temperature. Both of the correlations yield very close statistical performance in predicting the condenser heat rejection rate and the rate of total exergy destruction in the system.

Because the correlations result in accurate predictions, both of them can be used for predicting the performance parameters of automotive air conditioning systems. Accordingly, the performance of automotive air conditioning systems can be accurately determined by employing limited number of test results to find the coefficients in the correlations. Thus, engineering effort as well as time and funds can be saved.

REFERENCES

Alkan A. and Hosoz M., 2010a, Comparative Performance of an Automotive Air Conditioning System Using Fixed and Variable Capacity Compressors, *Int. J. Refrigeration*, 33, 487−495.

Alkan A. and Hosoz M., 2010b, Experimental Performance of an Automobile Air Conditioning System Using a Variable Capacity Compressor for Two Different Types of Expansion Devices, *Int. J. Vehicle Des.*, 152, 160–176.

Atik K., Aktaş A. and Deniz E., 2010, Performance Parameters Estimation of MAC by using Artificial Neural Network, *Expert Syst. Appl.*, 37, 5436–5442.

Belman-Flores J.M. and Ledesma S., 2015, Statistical Analysis of the Energy Performance of a Refrigeration System Working with R1234yf Using Artificial Neural Networks. *Appl. Therm. Eng.*, 82, 8–17.

Bhatti M., 1999, Evolution of Automotive Air Conditioning – Riding in Comfort: Part II, *ASHRAE J*, 41, 44−50.

Hemami T. L., 1999, *Development of Transient System Model of Mobile Air Conditioning System*, Ph.D. Thesis, University of Illinois, IL, USA.

Holman J. P., 2012, *Experimental Methods for Engineers*, McGraw-Hill, New York.

Hosoz M., Alkan A. and Ertunc H., M., 2013, Modelling of an Automotive Air Conditioning System using ANFIS, *Isı Bilim. Tek. Derg.*, 33, 1, 127–137.

Hosoz M. and Direk, M., 2006, Performance Evaluation of an Integrated Automotive Air Conditioning and Heat Pump System, *Energy Convers. Manage.*, 47, 545–559.

Hosoz M. and Ertunc H.M., 2006, Artificial Neural Network Analysis of an Automobile Air Conditioning System, *Energy Convers. Manage.*, 47, 1574–1587.

Kamar H. M., Ahmad R., Kamsah N.B. and Mustafa A. F. M., 2013, Artificial Neural Networks for Automotive Air-Conditioning Systems Performance Prediction, *Appl. Therm. Eng.*, 50, 63–70.

Kiatsiriroat T. and Euakit T., 1997, Performance Analyses of an Automobile Air-Conditioning System with R22/R124/R152a Refrigerant, *Appl. Therm. Eng*., 17, 1085–1097.

Lee Y. and Jung D., 2012, A Brief Performance Comparison of R1234yf and R134a in a Bench Tester for Automobile Applications, *Appl. Therm. Eng.*, 35, 240–242.

Moffat R.J., 1988, Describing the Uncertainties in Experimental Results, *Exp. Therm. Fluid Sci.*, 1, 3–17.

Navarro-Esbrí J., Mendoza-Miranda J.M., Mota-Babiloni A., Barragán-Cervera A. and Belman-Flores J.M., 2013, Experimental Analysis of R1234yf as a Drop-in Replacement for R134a in a Vapor Refrigerant System, *Int. J. Refrigeration*, 36, 870–880.

Ozgener O. and Hepbasli A., 2007, Modeling and Performance Evaluation of Ground Source (Geothermal) Heat Pump Systems, *Energ*. *Buildings*, 39, 66–75.

Qi Z., 2015, Performance Improvement Potentials of R1234yf Mobile Air Conditioning System, *Int. J. Refrigeration*, 58, 35–40.

Stoecker W.F. and Jones W.B., 1982, *Refrigeration & Air Conditioning*, McGraw-Hill, Singapore.

UNEP, 1987, *Montreal Protocol on Substances that Deplete the Ozone Layer, Final Act*, United Nations, New York, USA.

Vargas J.V.C. and Parise J.A.R., 1995, Simulation in Transient Regime of a Heat Pump with Closed-Loop and On–Off Control, *Int. J. Refrigeration*, 18, 235–243.

Wang C-C., 2014, System Performance of R-1234yf Refrigerant in Air-Conditioning and Heat Pump System - An Overview of Current Status, *Appl. Therm. Eng.*, 73, 1412–1420.

Yataganbaba A., Kilicarslan A. and Kurtbas I., 2015, Energy Analysis of R1234yf and R1234ze as R134a Replacements in a Two Evaporator Vapour Compression Refrigeration System, *Int. J. Refrigeration*, 60, 26–37.

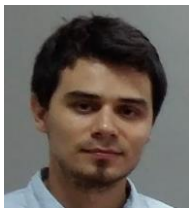

Mumin Celil ARAL received his BSc degree from Mechanical Engineering, Karadeniz Technical University in 2014. Then, he received his MSc degree from Automotive Engineering, Kocaeli University in 2016. His research interests lie in the area of automotive air conditioning systems, alternative refrigerants and modelling of condenser heat transfer.

Murat HOSOZ received his BSc degree from Mechanical Engineering, Uludag University in 1988; MSc and PhD degrees also from Mechanical Engineering, Istanbul Technical University in 1990 and 1999, respectively. He is currently a professor in the Department of Automotive Engineering, Kocaeli University. His research interests are automotive air conditioning systems, alternative refrigerants, refrigeration systems, thermal systems, internal combustion engines and modelling of heat transfer in automotive condensers, evaporators and radiators.

Mukhamad SUHERMANTO received his BSc degree from Automotive Education, Malang State University, Indonesia, in 2013. Then, he received his MSc degree from Automotive Engineering, Kocaeli University in 2016. He is currently working for an Indonesian university as a part-time instructer. His research interests lie in the area of automotive air conditioning and heat pump systems as well as alternative refrigerants.